

Parallel Coordinate Descent Newton Method for Efficient L_1 -Regularized Loss Minimization*

An Bian
ybian@inf.ethz.ch
ETH Zurich

Xiong Li
li.xiong@gmail.com
CNCERT

Yuncai Liu
whomliu@sjtu.edu.cn
Shanghai Jiao Tong University

Ming-Hsuan Yang
mhyang@ucmerced.edu
University of California, Merced

Abstract

The recent years have witnessed advances in parallel algorithms for large scale optimization problems. Notwithstanding the demonstrated success, existing algorithms that parallelize over features are usually limited by divergence issues under high parallelism or require data preprocessing to alleviate these problems. In this work, we propose a Parallel Coordinate Descent algorithm using *approximate* Newton steps (PCDN) that is guaranteed to converge globally without data preprocessing. The key component of the PCDN algorithm is the high-dimensional line search, which guarantees the global convergence with high parallelism. The PCDN algorithm randomly partitions the feature set into b subsets/bundles of size P , and sequentially processes each bundle by first computing the descent directions for each feature in parallel and then conducting P -dimensional line search to compute the step size. We show that (i) the PCDN algorithm is guaranteed to converge globally despite increasing parallelism; (ii) the PCDN algorithm converges to the specified accuracy ϵ within the limited iteration number of T_ϵ , and T_ϵ decreases with increasing parallelism. In addition, the data transfer and synchronization cost of the P -dimensional line search can be minimized by maintaining intermediate quantities. For concreteness, the proposed PCDN algorithm is applied to L_1 -regularized logistic regression and L_1 -regularized L_2 -loss SVM problems. Experimental evaluations on seven benchmark datasets show that the proposed PCDN algorithm exploits parallelism well and outperforms the state-of-the-art methods.

1. Introduction

High dimensional L_1 -minimization problems arise in a wide range of applications including sparse logistic regression [15], L_1 -regularized support vector machine (SVM) classification [4], image coding [11], and face recognition [23]. To solve L_1 -optimization

*Source code is available at <https://github.com/bianan/ParallelCDN>

problems efficiently, several algorithms based on coordinate gradient descent (CGD) [22], stochastic gradient [21], interior point [8] and trust region [12] have been developed, among which the Coordinate Descent Newton (CDN) [24] and improved GLM-NET [25] methods have demonstrated promising results for L_1 -regularized linear optimization problems.

Within the L_1 -optimization framework, large datasets with high dimensional features entail scalable and efficient parallel algorithms. Several methods perform parallelization over samples [9; 16; 26; 27] although usually there are more features than samples in L_1 -regularized problems. Richtárik et al. [17] show that randomized coordinate descent methods can be accelerated by parallelization for solving Lasso problems, and the work is further extended to distributed settings [14; 18]. In addition, Bradley et al. [2] propose the Shotgun CDN (SCDN) method for L_1 -regularized logistic regression by directly parallelizing the updates of features based on the CDN algorithm [24]. However, the SCDN method is not guaranteed to converge when the number of updated features in parallel is greater than a threshold, and thereby limits its ability of exploiting high parallelism. While this problem can be alleviated by preprocessing samples (e.g., feature clustering) to achieve higher parallelism [20], it requires additional computational overhead. The Accelerated Shotgun method [13] is a first-order algorithm without backtrack line search which has fast convergence. However, it can only deal with the objective functions without regularization terms. Scherrer et al. [19] present a generic framework for parallel coordinate descent methods which includes Shotgun, Greedy, Thread-Greedy and Coloring. Their empirical convergence and scalability tests do not favor any of these methods over the others, and no theoretical analysis is presented for the general framework.

In [1] Bian et al. present a high dimensional line search algorithm to ensure global convergence while performing parallel coordinate updates for L_1 -regularized logistic regression problem. While this method performs well, no analysis of convergence rate is presented. In this work, by further exploring the idea, we propose a generalized Parallel Coordinate Descent method using *approximate* Newton steps (PCDN) for generic L_1 -optimization problems, and present thorough theoretical analysis on the proposed method.

The contributions and novelty of this work are summarized as follows. We present theoretical analysis on the upper bound of the expected line search step in each iteration. We analyze the iteration complexity of the proposed PCDN algorithm and show that, for any bundle size P (i.e., parallelism), it is guaranteed to converge to a specified accuracy ϵ within T_ϵ iterations. The iteration number T_ϵ decreases with the increasing of parallelism (bundle size P). In addition, we show that in our implementation, the P -dimensional line search does not need to access all the training data on each thread and the synchronization cost of the P -dimensional line search can be minimized. Extensive experiments on L_1 -regularized classification and regression problems with real-world datasets demonstrate that the proposed PCDN

algorithm is a highly parallelized approach with guaranteed global convergence and fast convergence rate.

2. L_1 -Regularized Loss Minimization

For ease of presentation, we summarize the mathematical notations in Table 1.

Table 1: Mathematical notations in this work.

s, n	# training samples and # features
i, j	sample index and feature index
t	cumulative inner iteration index
k	outer iteration index
\mathbf{e}_j	indicator vector
$\ \cdot\ , \ \cdot\ _1$	2-norm and 1-norm
\mathcal{N}	$\{1, 2, \dots, n\}$, feature index set
$\mathcal{B} \subseteq \mathcal{N}$	feature index subset or “bundle”
$P = \mathcal{B} $	bundle size
$\mathbf{w} \in \mathbb{R}^n$	unknown vector of model weights
$\mathbf{X} \in \mathbb{R}^{s \times n}$	design matrix, whose i -th row is \mathbf{x}_i
(\mathbf{x}_i, y_i)	sample-label pair

Consider an unconstrained L_1 -regularized minimization problem over a training set $\{(\mathbf{x}_i, y_i)\}_{i=1}^s$ with the following general form:

$$\begin{aligned} \min_{\mathbf{w} \in \mathbb{R}^n} F(\mathbf{w}) &:= \min_{\mathbf{w} \in \mathbb{R}^n} c \sum_{i=1}^s \varphi(\mathbf{w}; \mathbf{x}_i, y_i) + \|\mathbf{w}\|_1 \\ &= \min_{\mathbf{w} \in \mathbb{R}^n} L(\mathbf{w}) + \|\mathbf{w}\|_1, \end{aligned} \quad (1)$$

where $L(\mathbf{w}) := c \sum_{i=1}^s \varphi(\mathbf{w}; \mathbf{x}_i, y_i)$ is the overall loss function; $\varphi(\mathbf{w}; \mathbf{x}_i, y_i)$ is a convex and non-negative loss function; and $c > 0$ is the regularization parameter. For L_1 -regularized logistic regression, the loss function is,

$$\varphi_{\log}(\mathbf{w}; \mathbf{x}_i, y_i) = \log(1 + e^{-y_i \mathbf{w}^\top \mathbf{x}_i}), \quad (2)$$

and for L_1 -regularized L_2 -loss SVM, the loss function is

$$\varphi_{\text{svm}}(\mathbf{w}; \mathbf{x}_i, y_i) = \max(0, 1 - y_i \mathbf{w}^\top \mathbf{x}_i)^2. \quad (3)$$

A number of algorithms have been proposed to solve these problems. We discuss two related solvers based on Coordinate Descent Newton [24] and its parallel variant, Shotgun CDN [2], in this section.

2.1 Coordinate Descent Newton

Based on the Coordinate Gradient Descent (CGD) method [22], Yuan et al. [24] demonstrate that the CDN method is efficient for solving large scale L_1 -regularized minimization. The overall procedure is summarized in Algorithm 1. Given the current

Algorithm 1: CDN [24]

```

1 initialize  $\mathbf{w}^0 = \mathbf{0}_{n \times 1}$ ;
2 for  $k = 0, 1, 2, \dots$  do
3   for all  $j \in \mathcal{N}$  do
4     compute  $d_j^k = d(\mathbf{w}^{k,j}; j)$  by solving (4);
5     find  $\alpha^{k,j} = \alpha(\mathbf{w}^{k,j}, d_j^k \mathbf{e}_j)$  by solving (6);
      // 1-dimensional line search
6      $\mathbf{w}^{k,j+1} \leftarrow \mathbf{w}^{k,j} + \alpha^{k,j} d_j^k \mathbf{e}_j$ ;
```

model \mathbf{w} , for the selected feature $j \in \mathcal{N}$, \mathbf{w} is updated in the direction $\mathbf{d}^j = d(\mathbf{w}; j)\mathbf{e}_j$, where²

$$d(\mathbf{w}; j) := \arg \min_d \{ \nabla_j L(\mathbf{w})d + \frac{1}{2} \nabla_{jj}^2 L(\mathbf{w})d^2 + |w_j + d| \}, \quad (4)$$

which has the following closed form solution,

$$d(\mathbf{w}; j) = \begin{cases} -\frac{\nabla_j L(\mathbf{w})+1}{\nabla_{jj}^2 L(\mathbf{w})} & \text{if } \nabla_j L(\mathbf{w}) \leq \nabla_{jj}^2 L(\mathbf{w})w_j, \\ -\frac{\nabla_j L(\mathbf{w})-1}{\nabla_{jj}^2 L(\mathbf{w})} & \text{if } \nabla_j L(\mathbf{w}) \geq \nabla_{jj}^2 L(\mathbf{w})w_j, \\ -w_j & \text{otherwise.} \end{cases} \quad (5)$$

The Armijo rule [3] is used to determine the step size. Let q be the line search step index, the step size $\alpha = \alpha(\mathbf{w}, \mathbf{d})$ is determined by

$$\alpha(\mathbf{w}, \mathbf{d}) := \max_{q=0,1,\dots} \{ \beta^q |F(\mathbf{w} + \beta^q \mathbf{d}) - F(\mathbf{w})| \leq \beta^q \sigma \Delta \}, \quad (6)$$

where $\beta \in (0, 1)$, $\sigma \in (0, 1)$, and

$$\Delta := \nabla L(\mathbf{w})^\top \mathbf{d} + \gamma \mathbf{d}^\top \mathbf{H} \mathbf{d} + \|\mathbf{w} + \mathbf{d}\|_1 - \|\mathbf{w}\|_1, \quad (7)$$

where $\gamma \in [0, 1)$ and $\mathbf{H} = \text{diag}(\nabla^2 L(\mathbf{w}))$.

This rule requires function evaluations in each line search step, straightforward implementation would need to access the whole design matrix \mathbf{X} for each function evaluation, which is intractable for parallel system with limited memory bandwidth. We will show in Section 3.1 that, this problem can be solved using implementation technique of retaining intermediate quantities, which also makes it possible to apply high-dimensional line search to our parallel algorithm.

2. For $L(\mathbf{w})$ that is not C^2 -smooth, e.g. the L_1 -regularized L_2 -loss SVM, use the generalized Hessian [24], which is denoted by $\nabla^2 L(\mathbf{w})$ with a little abuse of notation in this work.

Algorithm 2: Shotgun CDN for logistic regression [2]

```
1 choose  $\bar{P} \in [1, n/\rho + 1]$ , initialize  $\mathbf{w} = \mathbf{0}_{n \times 1}$ ;  
2 while not converged do  
3   in parallel on  $\bar{P}$  processors;  
4     choose  $j \in \mathcal{N}$  uniformly at random;  
5     obtain  $d_j = d(\mathbf{w}; j)$  by solving (4);  
6     find  $\alpha^j = \alpha(\mathbf{w}, d_j \mathbf{e}_j)$  by solving (6);  
7     // 1-dimensional line search  
8    $\mathbf{w} \leftarrow \mathbf{w} + \alpha^j d_j \mathbf{e}_j$ ;
```

2.2 SCDN for L_1 -Regularized Logistic Regression

The SCDN method [2] is developed to solve L_1 -regularized logistic regression problems. For presentation clarity, we summarize the main steps of the SCDN method in Algorithm 2. This method first determines the parallelism (number of parallel updates) \bar{P} , and then in each iteration updates the randomly picked \bar{P} features in parallel, where each feature update corresponds to one iteration in the inner loop of the CDN method (see Algorithm 1). However, the parallel updates for \bar{P} features increase the risk of divergence due to feature correlations. Bradley et al. [2] provide a problem-specific measure for the parallelization potential of the SCDN method based on the spectral radius ρ of $\mathbf{X}^\top \mathbf{X}$. With this measure, an upper bound $\bar{P} \leq n/\rho + 1$, is given to achieve speedups linear in \bar{P} . However, ρ can be very large for most large scale datasets (e.g., $\rho = 20, 228, 800$ for the `gisette` dataset with $n = 5000$ without column-wise normalization) and thus limits the parallelizability of SCDN. Clearly it is of great interest to develop algorithms with strong convergence guarantees under high parallelism for large scale L_1 -regularized minimization problems.

3. The Proposed PCDN Algorithm

As described in Section 2.2, the SCDN method is not guaranteed to converge when the number of features to be updated in parallel is greater than a threshold, i.e., $\bar{P} > n/\rho + 1$. To exploit higher parallelism, we propose a coordinate descent algorithm using multidimensional *approximate* Newton steps and high dimensional line search. When computing the multidimensional Newton descent direction of the second order approximation subproblem, we set the off-diagonal elements of the Hessian to zeros, such that we can compute the multidimensional approximate Newton descent direction by computing the corresponding one-dimensional Newton descent directions in parallel.

The main steps of the proposed PCDN method are summarized in Algorithm 3. In the k -th iteration of the outer loop, we randomly partition the feature index set

Algorithm 3: PCDN algorithm

```

1 choose  $P \in [1, n]$ , initialize  $\mathbf{w}^0 = \mathbf{0}_{n \times 1}$ ;
2 for  $k = 0, 1, 2, \dots$  do
3    $\{\mathcal{B}^{kb}, \mathcal{B}^{kb+1}, \dots, \mathcal{B}^{(k+1)b-1}\} \leftarrow$  random disjoint partitions of  $\mathcal{N}$  according
   to (8);
4   for  $t = kb, kb + 1, \dots, (k + 1)b - 1$  do
5      $\mathbf{d}^t \leftarrow \mathbf{0}_{n \times 1}$ ;
6     for all  $j \in \mathcal{B}^t$  in parallel do
7       obtain  $d_j^t = d(\mathbf{w}^t; j)$  by solving (4);
8     find  $\alpha^t = \alpha(\mathbf{w}^t, \mathbf{d}^t)$  by solving (6);
      //  $P$ -dimensional line search (see Algorithm 4 for detail)
9      $\mathbf{w}^{t+1} \leftarrow \mathbf{w}^t + \alpha^t \mathbf{d}^t$ ;

```

\mathcal{N} into b disjoint subsets in a Gauss-Seidel manner,

$$\mathcal{N} = \mathcal{B}^{kb} \cup \mathcal{B}^{kb+1} \cup \dots \cup \mathcal{B}^{(k+1)b-1}, \quad k = 0, 1, 2, \dots \quad (8)$$

where \mathcal{B} denotes a subset, i.e., a *bundle*, in this work; $P = |\mathcal{B}|$ is the bundle size; and $b = \lceil \frac{n}{P} \rceil$ is the number of bundles partitioned from \mathcal{N} . The PCDN algorithm sequentially processes each bundle by computing the approximate Newton descent direction in each iteration of the inner loop. In the t -th iteration³, the P -dimensional approximate Newton descent direction is computed by,

$$\mathbf{d}(\mathbf{w}; \mathcal{B}^t) \triangleq \arg \min_{\mathbf{d}} \left\{ \nabla_{\mathcal{B}^t} L(\mathbf{w}) \mathbf{d} + \frac{1}{2} \mathbf{d}^T \mathbf{H}_{\mathcal{B}^t} \mathbf{d} + \|\mathbf{w}_{\mathcal{B}^t} + \mathbf{d}\|_1 \right\},$$

where we only use the diagonal elements of the Hessian, i.e., $\mathbf{H}_{\mathcal{B}^t} \triangleq \text{diag}(\nabla_{\mathcal{B}^t}^2 L(\mathbf{w}))$, to make the computing of one-dimensional Newton descent direction independent of each other and enable the parallelization. That is,

$$\begin{aligned} \mathbf{d}(\mathbf{w}; \mathcal{B}^t) &= \arg \min_{\mathbf{d}} \left\{ \nabla_{\mathcal{B}^t} L(\mathbf{w}) \mathbf{d} + \frac{1}{2} \mathbf{d}^T \text{diag}(\nabla_{\mathcal{B}^t}^2 L(\mathbf{w})) \mathbf{d} \right. \\ &\quad \left. + \|\mathbf{w}_{\mathcal{B}^t} + \mathbf{d}\|_1 \right\} \\ &= \sum_{j \in \mathcal{B}^t} \left\{ \arg \min_d \nabla_j L(\mathbf{w}) d + \frac{1}{2} \nabla_{jj}^2 L(\mathbf{w}) d^2 + |w_j + d| \right\} \mathbf{e}_j \\ &= \sum_{j \in \mathcal{B}^t} d(\mathbf{w}; j) \mathbf{e}_j, \end{aligned} \quad (9)$$

3. Note that t is the cumulative iteration index, and refers to the inner loop in the following discussion of PCDN.

where (9) is from the definition of $d(\mathbf{w}; j)$ in (4). In the t -th iteration, we first compute the one-dimensional descent directions d_j^t (step 7) for P features in \mathcal{B}^t in parallel, which constitutes the P -dimensional descent direction \mathbf{d}^t ($d_j^t = 0, \forall j \notin \mathcal{B}^t$). We then use the P -dimensional Armijo line search (step 8) to compute the step size α^t of the bundle along \mathbf{d}^t , and update the model for the features in \mathcal{B}^t (step 9).

The PCDN algorithm is different from the SCDN method in three aspects: (1) PCDN randomly partitions the feature set into bundles and performs parallelization for features of each bundle, while SCDN does not; (2) PCDN performs P -dimensional line search for a bundle of features while SCDN performs 1-dimensional line search for each feature; (3) PCDN is guaranteed to reach global convergence for high parallelism whereas SCDN is not.

The P -dimensional line search is the key procedure that guarantees the convergence of PCDN. With P -dimensional line search, the objective function $F(\mathbf{w})$ in (1) is ensured to be non-increasing for any bundle \mathcal{B}^t (See Lemma 1(c) of Section 4). In general, the P -dimensional line search tends to have a large step size if the features in \mathcal{B}^t are less correlated, and a small step size otherwise.

The bundle size P controls the ratio between computation and data communication. From Algorithm 3, in each outer iteration, it updates n features (computation) while conducts $\lceil \frac{n}{P} \rceil$ times high-dimensional line search (which requires synchronization and communication). The bundle size P affects convergence rate (See Theorem 2) as well, and the choice of P is discussed at length in Section 5.1.

The PCDN algorithm can better exploit parallelism than the SCDN method. In step 7 of Algorithm 3, the descent direction for P features can be computed in parallel on P threads. We show in Section 4 that the proposed PCDN algorithm is guaranteed to reach global convergence, for any $P \in [1, n]$. Therefore, the bundle size P which measures the parallelism can be large when the number of features n is large. In contrast, for SCDN, the number of parallel updates \bar{P} is no more than $n/\rho + 1$ [2].

3.1 PCDN on Multicore

We use the technique of retaining intermediate quantities, in a way similar to the that in [6], by which two crucial implementation issues are addressed simultaneously. First, due to limited memory bandwidth, we lower data transfer by ensuring that one core is only needed to access data of one feature. Second, we lower synchronization cost of the P -dimensional line search such that the PCDN algorithm only requires one implicit barrier synchronization in each iteration. In our implementation, the line search procedure (6) does not require direct function value evaluation and thus avoids accessing all the training data on each core. Namely, the core processing on the j -th feature only needs to access the data related to the j -th feature (i.e., the j -th column \mathbf{x}^j of the design matrix \mathbf{X}).

Without loss of generality, let us take logistic regression for instance. We retain intermediate quantities $\mathbf{d}^\top \mathbf{x}_i$ and $e^{\mathbf{w}^\top \mathbf{x}_i}$ ($i = 1, \dots, s$). For the Armijo line search (summarized in Algorithm 4), we use the descent condition expressed by intermediate

Algorithm 4: Efficient high dimensional line Search (logistic regression here for example)

```

1 compute  $\mathbf{d}^\top \mathbf{x}_i, i = 1, \dots, s$ ; // parallel
2 for  $q = 0, 1, 2, \dots$  do
3   if (10) is satisfied then
4      $\mathbf{w} \leftarrow \mathbf{w} + \beta^q \mathbf{d}$ ;
5      $e^{\mathbf{w}^\top \mathbf{x}_i} \leftarrow e^{\mathbf{w}^\top \mathbf{x}_i} e^{\beta^q \mathbf{d}^\top \mathbf{x}_i}$ ; // parallel
6     break;
7   else
8      $\Delta \leftarrow \beta \Delta$ ;
9      $\mathbf{d}^\top \mathbf{x}_i \leftarrow \beta \mathbf{d}^\top \mathbf{x}_i, i = 1, \dots, s$ ; // parallel

```

quantities in the following equation,

$$\begin{aligned}
F(\mathbf{w} + \beta^q \mathbf{d}) - F(\mathbf{w}) &= \|\mathbf{w} + \beta^q \mathbf{d}\|_1 - \|\mathbf{w}\|_1 + \\
c \left(\sum_{i=1}^s \log \left(\frac{e^{(\mathbf{w} + \beta^q \mathbf{d})^\top \mathbf{x}_i} + 1}{e^{(\mathbf{w} + \beta^q \mathbf{d})^\top \mathbf{x}_i} + e^{\beta^q \mathbf{d}^\top \mathbf{x}_i}} \right) + \beta^q \sum_{i: y_i = -1} \mathbf{d}^\top \mathbf{x}_i \right) & \quad (10) \\
\leq \sigma \beta^q (\nabla L(\mathbf{w}))^\top \mathbf{d} + \gamma \mathbf{d}^\top \mathbf{H} \mathbf{d} + \|\mathbf{w} + \mathbf{d}\|_1 - \|\mathbf{w}\|_1
\end{aligned}$$

which is equivalent to the descent condition in (6). More specifically, in Algorithm 3, the core processing the j -th feature only needs to access \mathbf{x}^j twice in the t -th iteration.

For the first time at step 7 of Algorithm 3, \mathbf{x}^j is accessed and the retained $e^{\mathbf{w}^\top \mathbf{x}_i}$ is used to compute the j -th gradient and Hessian,

$$\begin{aligned}
\nabla_j L(\mathbf{w}) &= c \sum_{i=1}^s (\tau(y_i \mathbf{w}^\top \mathbf{x}_i) - 1) y_i x_{ij}, \\
\nabla_{jj}^2 L(\mathbf{w}) &= c \sum_{i=1}^s \tau(y_i \mathbf{w}^\top \mathbf{x}_i) (1 - \tau(y_i \mathbf{w}^\top \mathbf{x}_i)) x_{ij}^2,
\end{aligned} \quad (11)$$

where $\tau(s) = \frac{1}{1+e^{-s}}$. They are then used to compute $d(\mathbf{w}; j)$ in (4). For the second time at step 8 of Algorithm 3, \mathbf{x}^j is accessed and \mathbf{d} is used to update $\mathbf{d}^\top \mathbf{x}_i$, which is then used with $e^{\mathbf{w}^\top \mathbf{x}_i}$ to check the descent condition in (10).

The proposed PCDN algorithm requires much less time for each outer iteration than the CDN method, which is analyzed in Section B of the appendix.

4. Convergence of PCDN

In this section, we analyze the convergence of the proposed PCDN algorithm from three aspects: convergence of P -dimensional line search, global convergence and convergence rate. For presentation clarity, we first discuss the main results and present

all the proofs in the appendix. Before analyzing the convergence of PCDN, we present the following lemma.

Lemma 1. *Let $\{\mathbf{w}^t\}$, $\{\mathbf{d}^t\}$, $\{\alpha^t\}$ as well as $\{\mathcal{B}^t\}$ be sequences generated by Algorithm 3, $\bar{\lambda}(\mathcal{B}^t)$ be the maximum element of $(\mathbf{X}^\top \mathbf{X})_{jj}$ where $j \in \mathcal{B}^t$, and λ_k be the k -th minimum element of $(\mathbf{X}^\top \mathbf{X})_{jj}$ where $j \in \mathcal{N}$. The following results hold.*

- (a) $\mathbf{E}_{\mathcal{B}^t}[\bar{\lambda}(\mathcal{B}^t)]$ is monotonically increasing with respect to P ; $\mathbf{E}_{\mathcal{B}^t}[\bar{\lambda}(\mathcal{B}^t)]$ is constant with respect to P if λ_i is constant (i.e., $\lambda_1 = \dots = \lambda_n$); $\mathbf{E}_{\mathcal{B}^t}[\bar{\lambda}(\mathcal{B}^t)]/P$ is monotonically decreasing with respect to P .
- (b) For L_1 -regularized logistic regression in (2) and L_1 -regularized L_2 -loss SVMs in (3), the diagonal elements of the (generalized) Hessian of the loss function $L(\mathbf{w})$ have positive lower bound \underline{h} and upper bound \bar{h} , and the upper bound only depends on the design matrix \mathbf{X} . That is, $\forall j \in \mathcal{N}$,

$$\nabla_{jj}^2 L(\mathbf{w}) \leq \theta c (\mathbf{X}^\top \mathbf{X})_{jj} = \theta c \sum_{i=1}^s x_{ij}^2, \quad (12)$$

$$0 < \underline{h} \leq \nabla_{jj}^2 L(\mathbf{w}) \leq \bar{h} = \theta c \bar{\lambda}(\mathcal{N}), \quad (13)$$

where $\theta = \frac{1}{4}$ for logistic regression and $\theta = 2$ for L_2 -loss SVM.

- (c) The objective $\{F(\mathbf{w}^t)\}$ is non-increasing and Δ^t (7) in the Armijo line search rule satisfies

$$\Delta^t \leq (\gamma - 1) \mathbf{d}^{t\top} \mathbf{H}^t \mathbf{d}^t, \quad (14)$$

$$F(\mathbf{w}^t + \alpha^t \mathbf{d}^t) - F(\mathbf{w}^t) \leq \sigma \alpha^t \Delta^t \leq 0. \quad (15)$$

We note that Lemma 1(a) is used to analyze the iteration number T_ϵ given the expected accuracy ϵ , Lemma 1(b) is used to prove Theorem 1 and 2. Lemma 1(c) ensures the descent of the objective theoretically and gives an upper bound for Δ^t in the Armijo line search, and is used to prove Theorem 1 and 2. Note that the upper bound $(\gamma - 1) \mathbf{d}^{t\top} \mathbf{H}^t \mathbf{d}^t$ is only related to the second order measurement.

Theorem 1 (Convergence of P -dimensional line search). *Let $\{\mathcal{B}^t\}$ be a sequence generated by Algorithm 3, and $\bar{\lambda}(\mathcal{B}^t) = \max\{(\mathbf{X}^\top \mathbf{X})_{jj} \mid j \in \mathcal{B}^t\}$. The P -dimensional line search converges in finite steps, and the expected line search step number in each iteration is bounded by*

$$\begin{aligned} \mathbf{E}[q^t] \leq & 1 + \log_{\beta^{-1}} \frac{\theta c}{2\underline{h}(1 - \sigma + \sigma\gamma)} \\ & + \frac{1}{2} \log_{\beta^{-1}} P + \log_{\beta^{-1}} \mathbf{E}[\bar{\lambda}(\mathcal{B}^t)], \end{aligned} \quad (16)$$

where the expectation is with respect to the random choice of \mathcal{B}^t ; q^t is the line search step number in the t -th iteration; $\beta \in (0, 1)$, $\sigma \in (0, 1)$ and $\gamma \in [0, 1)$ are parameters of the Armijo rule (6); θ and \underline{h} is in Lemma 1(b).

As $\mathbf{E}[\bar{\lambda}(\mathcal{B}^t)]$ is monotonically increasing with respect to P (Lemma 1(a)), Theorem 1 dictates that the upper bound of $\mathbf{E}[q^t]$ (the expected line search step number in each iteration) increases with the bundle size P . Since more line search steps lead to smaller step size (α), Theorem 1 is consistent with the intuition that smaller step size is used when features inside a bundle are more correlated.

Global convergence of PCDN. In Section A.5 of the appendix, we prove the global convergence of PCDN by connecting it to the general framework in [22]. By proving that all assumptions are satisfied, we show that, assuming that $\{\mathbf{w}^t\}$ is the sequence generated by Algorithm 3, then any limit point of $\{\mathbf{w}^t\}$ is an optimum. This analysis guarantees that the PCDN algorithm converges globally for any bundle size $P \in [1, n]$ (i.e., without regard to the level of parallelism).

Theorem 2 (Convergence rate of PCDN). *Assume \mathbf{w}^* minimize (1); $\{\mathbf{w}^t\}$ and $\{\mathcal{B}^t\}$ be sequences generated by Algorithm 3; $\bar{\lambda}(\mathcal{B}^t) := \max\{(\mathbf{X}^\top \mathbf{X})_{jj} \mid j \in \mathcal{B}^t\}$ and \mathbf{w}^T be the output of Algorithm 3 after $T + 1$ iterations. Then,*

$$\mathbf{E}[F(\mathbf{w}^T) - F(\mathbf{w}^*)] \leq \frac{n\mathbf{E}[\bar{\lambda}(\mathcal{B}^t)]}{P(T+1)} \cdot \frac{\theta c}{2\xi} \left[\|\mathbf{w}^*\|^2 + \frac{F(\mathbf{0})}{\sigma(1-\gamma)\underline{h}} \right],$$

where the expectation is computed with respect to random choice of \mathcal{B}^t ; $\sigma \in (0, 1)$ and $\gamma \in [0, 1)$ are parameters in the Armijo rule (6). In addition, θ as well as \underline{h} (positive lower bound of $\nabla_{jj}^2 L(\mathbf{w})$) are given in Lemma 1(b), and $\mathbf{E}[\bar{\lambda}(\mathcal{B}^t)]$ is determined by the bundle size P and design matrix X ; ξ is a positive constant.

Based on Theorem 2, we obtain the upper bound (T_ϵ^{up}) of the iteration number T_ϵ satisfying a specified accuracy ϵ :

$$\begin{aligned} T_\epsilon &\leq \frac{n\mathbf{E}[\bar{\lambda}(\mathcal{B}^t)]}{P\epsilon} \cdot \frac{\theta c}{2\xi} \left[\|\mathbf{w}^*\|^2 + \frac{F(\mathbf{0})}{\sigma(1-\gamma)\underline{h}} \right] \\ &:= T_\epsilon^{\text{up}} \propto \frac{\mathbf{E}[\bar{\lambda}(\mathcal{B}^t)]}{P\epsilon}, \end{aligned} \tag{17}$$

which means that the proposed PCDN algorithm achieves speedups linear in the bundle size P compared to the CDN method if $\mathbf{E}[\bar{\lambda}(\mathcal{B}^t)]$ remains constant⁴. In general, $\mathbf{E}[\bar{\lambda}(\mathcal{B}^t)]$ increases with respect to P (from Lemma 1(a)), and thus makes the speedup sublinear. Furthermore, since $\mathbf{E}[\bar{\lambda}(\mathcal{B}^t)]/P$ decreases with respect to P from Lemma 1(a), T_ϵ^{up} decreases with respect to P , and so does T_ϵ . Thus the PCDN algorithm requires fewer iterations with larger bundle size P to converge to ϵ accuracy.

To verify the upper bound T_ϵ^{up} (17) of the iteration number T_ϵ for a given accuracy ϵ , we set $\epsilon = 10^{-3}$ and show the iteration number T_ϵ as a function of the bundle size

4. If we perform feature-wise normalization over the training data X to ensure $\lambda_1 = \lambda_2 = \dots = \lambda_n$, then $\mathbf{E}[\bar{\lambda}(\mathcal{B}^t)]$ remains constant according to Lemma 1(a).

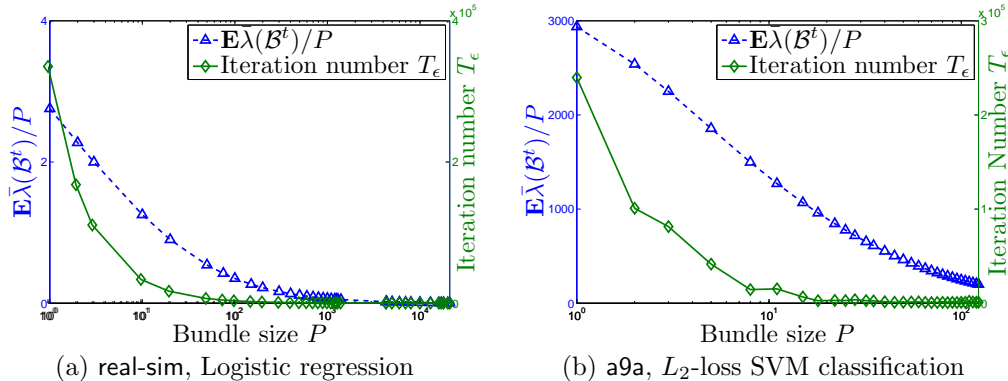


Figure 1: $\mathbf{E}[\bar{\lambda}(\mathcal{B}^t)]/P$ and T_ϵ as a function of bundle size P .

P in Figure 1, where two document datasets, **a9a** and **real-sim** (See Section 5.1 for details about the datasets) are used. Since T_ϵ^{up} is proportional to $\mathbf{E}[\bar{\lambda}(\mathcal{B}^t)]/P$, we plot $\mathbf{E}[\bar{\lambda}(\mathcal{B}^t)]/P$ instead of T_ϵ^{up} in Figure 1. The results match the upper bound in (17): for given ϵ , T_ϵ (solid green lines) is positively correlated with $\mathbf{E}[\bar{\lambda}(\mathcal{B}^t)]/P$ (dotted blue lines). In addition, T_ϵ decreases with respect to P . These results show that with larger bundle size P , fewer iterations are needed by the PCDN algorithm to converge to ϵ accuracy.

5. Experiments

In this section we present experimental results of the proposed PCDN algorithm, with comparisons to the state-of-the-art methods on L_1 -regularized loss minimization problems using several benchmark datasets.

5.1 Experimental Setup

Datasets. Seven benchmark datasets⁵ are used in our experiments and the characteristics are summarized in Table 2. The **news20**, **rcv1**, **a9a** and **real-sim** datasets consist of document data points that are normalized to unit vectors. The **a9a** dataset is from UCI data repository, and the **gissette** set consists of handwriting digit data points from the NIPS 2003 feature selection challenge where features are linearly scaled to the $[-1, 1]$ interval. The **kdda** dataset has been used for the KDD Cup 2010 data mining competition. The **webspam** dataset is the collection of Web pages that are created to manipulate search engines and deceive Web users.

Bundle Size Choice. For each dataset, the optimal bundle size P^* under which the PCDN algorithm achieves minimum runtime is determined as follows. For Al-

5. The datasets are available at <http://www.csie.ntu.edu.tw/~cjlin/libsvmtools/datasets>.

Table 2: Summary of datasets: s is The number of non-zero elements (NNZs) in training data is denoted by “train NNZ”; the average number of NNZs in the data corresponding to each feature is “NNZ/feature” denotes; “spa.” means train data sparsity, which is the ratio of zero elements in \mathbf{X} ; “ c^* SVM” and “ c^* logistic” denote the best regularization parameter c^* for L_2 -loss SVM and logistic regression, respectively, which are determined according to [24].

Dataset	s	n	train NNZ	NNZ/feature	spa./%	c^* SVM	c^* logistic
a9a	26,049	123	361,278	2,937	88.72	0.5	2.0
real-sim	57,848	20,958	2,968,110	142	99.76	1.0	4.0
news20	15,997	1,355,191	7,281,110	5	99.97	64.0	64.0
gisette	6,000	5,000	29,729,997	5,946	0.9	0.25	0.25
rcv1	541,920	47,236	39,625,144	839	99.85	1.0	4.0
kdda	8,407,752	20,216,830	305,613,510	15	99.99	1.0	1.0
webspam	280,000	16,609,143	1,043,724,776	63	99.9775	64.0	64.0

gorithm 3, the expected runtime of the t -th inner iteration of PCDN $\text{time}(t)$ can be approximated by

$$\mathbf{E}[\text{time}(t)] \approx (P/\#\text{thread}) \cdot t_{dc} + \mathbf{E}[q^t] \cdot t_{ls}, \quad (18)$$

where the expectation is based on a random choice of \mathcal{B}^t ; $\#\text{thread}$ is the number of threads used by PCDN and fixed to be 23 in our experiments; t_{dc} is the time for computing the descent direction (step 7 in Algorithm 3); t_{ls} is the time for a step of P -dimensional line search, which is approximately constant with varying P (as shown in Section B of the appendix).

Table 3: Optimal bundle size P^* for each dataset. $\#\text{thread} = 23$. The second row shows P^* for logistic regression, the third row shows P^* for L_2 -loss SVM.

a9a	real-sim	news20	gisette	rcv1	kdda	webspam
123	1250	400	20	1600	29500	31750
85	500	150	15	350	95000	86000

As $\mathbf{E}[q^t]$ increases with respect to the bundle size P (based on Theorem 1), $\mathbf{E}[\text{time}(t)]$ increases with respect to P based on (18). In addition, as the PCDN algorithm requires fewer iterations for larger P to converge to ϵ accuracy (from (17) in Section 4), it is essential to make a trade-off between the increasing runtime per iteration $\mathbf{E}[\text{time}(t)]$ and the decreasing iteration number T_ϵ to select the optimal bundle size P^* . In practice, we run PCDN with varying P . Figure 2 shows the training time as a function of bundle size P for the `real-sim` dataset and the optimal bundle

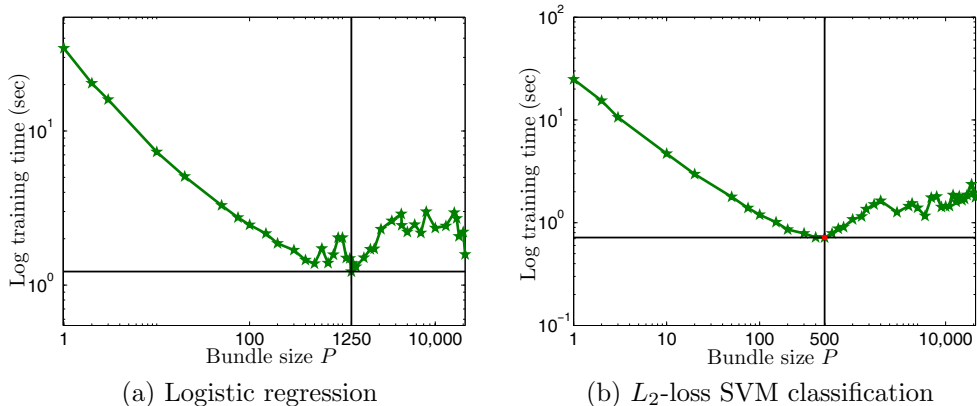


Figure 2: Training time v.s. bundle size P for the `real-sim` dataset with stopping criteria $\epsilon = 10^{-3}$, the intersection of the horizontal and vertical black line shows the optimal bundle size P^* .

size P^* can be determined. In this work, we empirically select the optimal P^* for each dataset (See Table 3).

We note that it is not necessary to obtain the optimal P to achieve significant speedup, as a wide range of P will suffice to achieve the same goal in practice. As shown in Figure 2(a), when P is greater than 500, it achieves considerable speedup higher than SCDN (5 times faster than SCDN for $P=500$). For a new dataset, one can first select a relatively large P (about 5% of #features) with the most relaxed stopping criteria for a pilot experiment, and then adjust P for best performance when necessary.

Evaluated Methods. We evaluate the proposed PCDN algorithm against the state-of-the-art L_1 -regularized optimization approaches, including newGLMNET [25], CDN [24], Shotgun-CDN (SCDN)⁶ [2], interior-point method (IPM) [8] and trust region Newton (TRON) [12] methods with C/C++ implementations. For the Armijo line search procedure (6) in the PCDN, CDN and SCDN methods, we set $\sigma = 0.01$, $\gamma = 0$ and $\beta = 0.5$ for fair comparisons. The OpenMP library is used for parallel programming. The stopping criteria used in the experiments are similar to the outer stopping condition used in [25].

The source code of the proposed PCDN algorithm will be made available to the public, and the implementation details are listed below:

6. Since the experimental validation in [2] has shown that SCDN is much faster than the SGD-type algorithms (including SGD, Parallel SGD [16; 26], and SMIDAS [21]) for datasets with more features, and SCDN performs well on datasets with more samples than features, we only compare the PCDN algorithm with the SCDN scheme here. The SCDN algorithm is also a competitive representative of the generic parallel coordinate descent algorithms in [19].

- CDN: we implement this method based on the source code in the LIBLINEAR⁷ toolbox. Since the shrinking procedure cannot be performed inside the parallel loop of the SCDN and PCDN methods, we use an equivalent implementation of the CDN scheme for fair comparisons, where the shrinking procedure is modified such that it is consistent with the other parallel algorithms.
- SCDN: We set $\bar{P} = 8$ for the SCDN method following Bradley et al. [2].
- PCDN: We implement this algorithm with conditions consistent with all other methods.
- TRON: We set $\sigma = 0.01$ and $\beta = 0.1$ in the projected line search according to Yuan et al. [24]. We use it as baseline algorithm for L_2 -loss SVM.
- newGLMNET: We use the same setting and implementation provided by Yuan et al. [25]. Since it is outperformed by CDN for L_2 -loss SVM, we only use it as baseline algorithm for logistic regression experiments.
- IPM: We use the source code⁸ and default settings in [8]. We use it as a baseline interior-point algorithm for logistic regression.

Platform. All experiments are carried out on a 64 bit machine with Intel Xeon 2.4 GHz CPU and 64 GB main memory. We set `#thread = 23` for PCDN on a 24-core machine, which is far less than the optimal bundle size P^* given in Table 3. We note that the descent direction (step 7 in Algorithm 3) of the PCDN algorithm can be fully parallelized on several hundreds even to thousands of threads.

5.2 L_1 -Regularized L_2 -Loss SVM

Figure 3 shows the runtime performance of the PCDN, CDN and TRON methods with the best regularization parameter c^* (determined based on Yuan et al. [24]) and varying stopping criteria ϵ (equivalent for three solvers). Experimental results show that the proposed PCDN algorithm performs favorably against the other methods. As a feature-based parallel algorithm, the proposed PCDN solver performs well for sparse datasets with more features as shown by the results on the `rcv1` and `news20` datasets, which are very sparse (training data sparsity, defined by the ratio of zero elements in design matrix \mathbf{X} and explained in Table 2, is 99.85% and 99.97%, respectively) with a large number of features (47,236 and 1,355,191). In such cases, the PCDN algorithm performs well against the TRON method. For the `news20` dataset, the PCDN solver is 29 times faster than TRON method and 18 times faster than CDN approach. We note that for the `a9a` dataset, the PCDN solver is sometimes slightly slower than the TRON method since it is a relatively dense dataset with fewer features than samples (only 123 features with 26,049 samples).

7. liblinear version 1.7, <http://www.csie.ntu.edu.tw/~cjlin/liblinear/>.

8. version 0.8.2, http://www.stanford.edu/~boyd/l1_logreg/

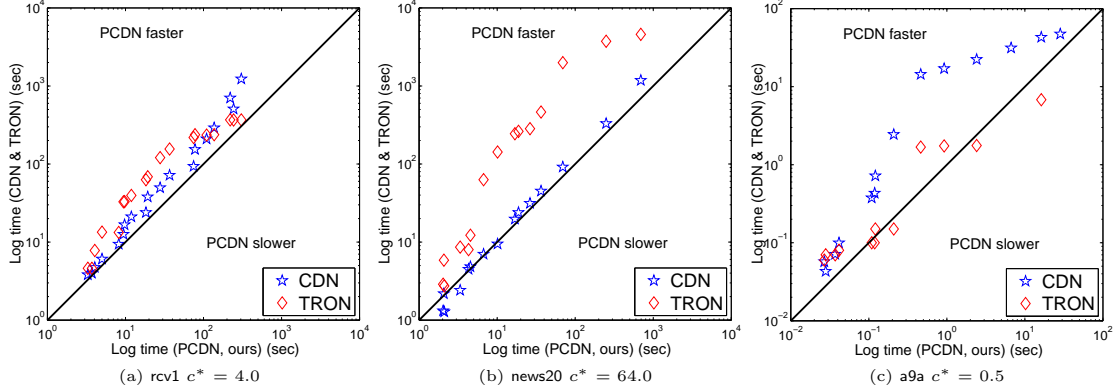


Figure 3: Runtime comparisons for L_2 -loss SVM classification where each marker compares a solver with PCDN on one dataset. The y -axis and x -axis show the runtime of a solver as well as PCDN on the same problem. Markers above the diagonal line indicate that PCDN is faster.

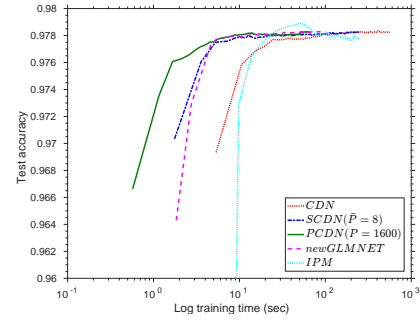
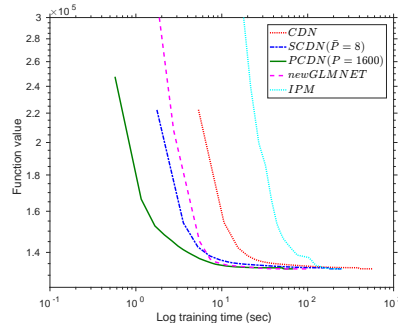
5.3 L_1 -Regularized Logistic Regression

We compare the runtime performance of the PCDN algorithm with the newGLMNET, IPM, SCDN and CDN methods on L_1 -regularized logistic regression with a bias term. Figure 4 shows the trace of function value (row 1) and test accuracy (row 2) with respect to the log runtime. Overall, the PCDN solver performs favorably against the other methods where the best speedup over the CDN method is 17.49 (with $\#thread = 23$). The speedup can be higher if more threads are used. For the *rcv1* dataset in Figure 4(a), the bundle size which reflects parallelism of PCDN is as high as 1,600.

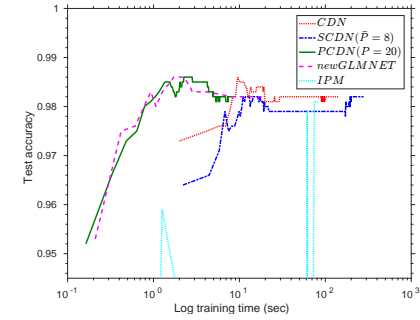
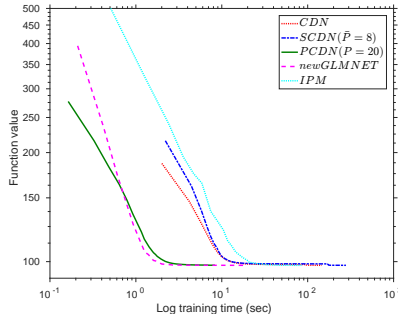
For the *gisette* dataset shown in Figure 4(b), the SCDN method is slower than the CDN scheme. This can be attributed to that the SCDN method is sensitive to correlation among features. Note that for *gisette* with 6,000 features the optimal P^* for PCDN is only 20, which also indicates the high correlation among features. For the *kdda* dataset, the computational load for IPM is prohibitively long, and not included in Figure 4(d). Despite the required runtime, the IPM method achieves higher accuracy on the *rcv1* and *real-sim* datasets.

Figure 4(e) shows that the PCDN performs favorably against the state-of-the-art methods on the large *webspam* dataset which consists of 1,043,724,776 non-zero elements. For the *kdda* dataset, the PCDN algorithm is slower than the SCDN method in the beginning but converges faster than the others in the end as shown in Figure 4(d). Except for the correlation among features and memory bandwidth limit, another issue that would significantly affect the performance of PCDN is the workload of the parallel threads. For the PCDN algorithm, each thread first processes one feature of the data, and then switches to the next feature. Thus, the parallel processing time

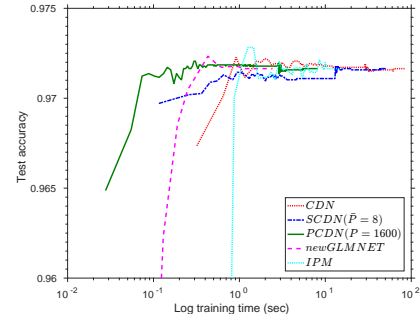
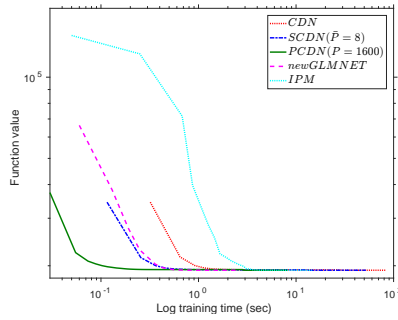
(a) rcv1 $\epsilon = 10^{-3}$



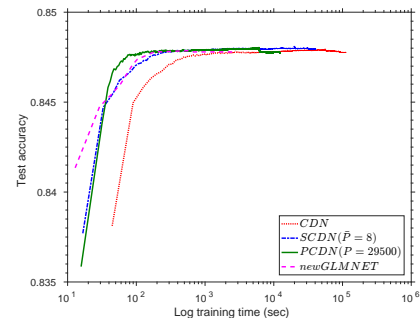
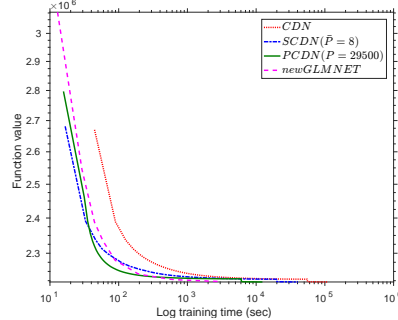
(b) gisette $\epsilon = 10^{-4}$



(c) real-sim $\epsilon = 10^{-6}$



(d) kdda $\epsilon = 3.7 * 10^{-3}$



(e) webspam $\epsilon = 10^{-2}$

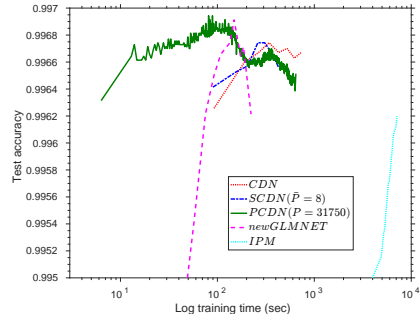
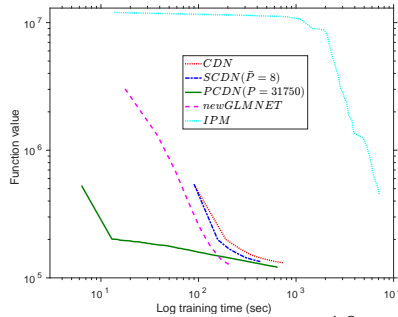


Figure 4: Runtime performance of PCDN, newGLMNET, SCDN, IPM and CDN for logistic regression. First column: function value. Second column: test accuracy.

of PCDN, which contributes to the acceleration, is proportional to the workload of the parallel threads. The workload of each thread is approximately proportional to the number of non-zero elements (NNZs) of the data corresponding to the feature being processed. To verify that, we compute the average number of NNZs per feature (NNZ/feature column in Table 2), and show that there are only 15 NNZs/feature in the `kdda` dataset, while there are 63 NNZs/feature in the `webspam` dataset. These results explain the performance difference of the PCDN algorithm on these two large datasets.

5.4 Scalability of PCDN

We also evaluate the scalability of PCDN in two aspects: whether PCDN can maintain the speed-up when the data size is increased, and whether PCDN can achieve better speed-up when the available computing resource (e.g., number of cores) is increased.

To analyze the effect of data size, we maintain all the other factors, e.g., correlation among features, the same in the experiments. To this end, we duplicate the samples to create datasets from 100% of original size to 2000%. Figure 5 shows the scalability over different number of cores and data size.

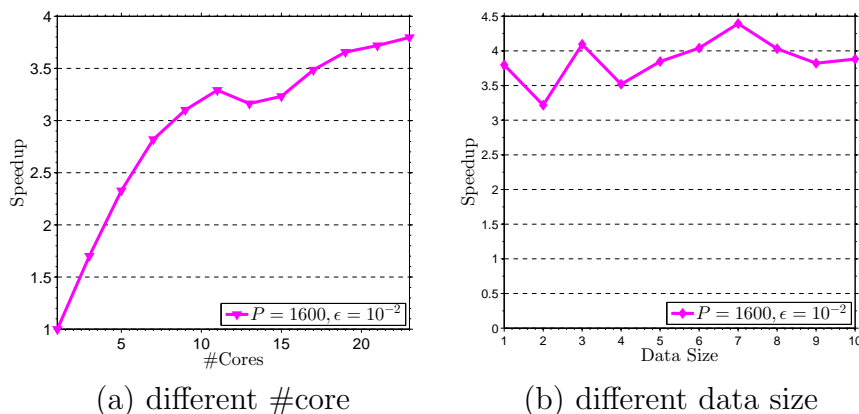


Figure 5: Speedup of PCDN on the `rcv1` dataset.

Effect of Number of Cores. Figure 5(a) shows that the speedup of the PCDN algorithm is larger at the beginning when the number of cores is increased (i.e., the parallel efficiency decreases with more parallelism) which can be explained by the Amdahl’s law: First, as the number of cores increase, the parallelized part takes less and less time. However, the serial part takes approximately the same constant time. Second, with more cores, there is increasing parallelization overhead, e.g., more data transfer, and thereby lowering parallel efficiency.

Effect of Data Size. Figure 5(b) shows that the speedup is approximately constant with larger data size, which shows the weak scaling property of parallel algorithms.

It is noteworthy that for very large dataset, the size of the data for each feature is also quite large that it may exceed the memory bandwidth.

5.5 Discussions

The high dimensional line search plays the key role in ensuring global convergence of PCDN. In this work, we use the Armijo line search as a specific realization, and it is worth exploring other ways to perform the line search. In addition, the computational cost of line search can be further reduced by deriving the (approximate) optimal line search step number, as what is performed for solving the dual linear SVM problem in [10].

The bundle size P controls the ratio between computation and communication, and thus affecting the running time of PCDN. Although we present an empirical method to choose a good P in Section 5.1, it is of great interest to develop a principled approach to determine the optimal value for P .

Another direction to pursue is to extend the PCDN algorithm within a distributed framework in a way similar to the Parallel SGD [27] and Downpour SGD [5] methods, to deal with very large datasets with lots of samples, that do not fit into one single machine. This can be achieved by first randomly distributing training data of different samples to different machines (i.e., parallelizing over samples), and applying the PCDN algorithm over a subset (i.e., parallelizing over features) on each machine, and aggregating all the models in the end. As a shared memory parallel algorithm, the PCDN algorithm can also be implemented with the stale synchronous parallel model [7] to achieve better performance.

6. Concluding Remarks

We propose an algorithm termed Parallel Coordinate Descent with *approximate* Newton step, with strong convergence guarantee, fast convergence rate and high parallelism for L_1 -regularized minimization problems. We show that the seemingly expensive high dimensional line search can be calculated efficiently with the implementation technique of maintaining intermediate quantities, which also minimizes the data transfer and synchronization cost of PCDN.

The PCDN can be *generalized* to solve the problems of minimizing the sum of a convex twice differentiable loss term and a separable regularization term. Thus, it allows L_1 (lasso), L_2 (ridge regression), and mixtures of the two penalties (elastic net). Experimental results on several benchmark datasets show that the proposed PCDN algorithm performs favorably against several state-of-the-art methods for L_1 -regularized optimization problems.

Acknowledgments

The authors would like to thank Hongyuan Zha, Xiangfeng Wang, Martin Takáč and Martin Jaggi for their valuable comments and suggestions to improve this work. This research was partially supported by the Max Planck ETH Center for Learning Systems

References

- [1] Yatao Bian, Xiong Li, Mingqi Cao, and Yuncai Liu. Bundle cdn: A highly parallelized approach for large-scale l1-regularized logistic regression. In *ECML/PKDD*, pages 81–95, 2013.
- [2] Joseph K. Bradley, Aapo Kyrola, Danny Bickson, and Carlos Guestrin. Parallel coordinate descent for l1-regularized loss minimization. In *ICML*, pages 321–328, 2011.
- [3] JamesV. Burke. Descent methods for composite nondifferentiable optimization problems. *Mathematical Programming*, 33(3):260–279, 1985.
- [4] Kai-Wei Chang, Cho-Jui Hsieh, and Chih-Jen Lin. Coordinate descent method for large-scale l2-loss linear support vector machines. *Journal of Machine Learning Research*, 9:1369–1398, 2008.
- [5] Jeffrey Dean, Greg S. Corrado, Rajat Monga, Kai Chen, Matthieu Devin, Quoc V. Le, Mark Z. Mao, Marc A. Ranzato, Andrew Senior, Paul Tucker, Ke Yang, and Andrew Y. Ng. Large Scale Distributed Deep Networks. In *NIPS*, 2012.
- [6] Rong-En Fan, Kai-Wei Chang, Cho-Jui Hsieh, Xiang-Rui Wang, and Chih-Jen Lin. Liblinear: A library for large linear classification. *Journal of Machine Learning Research*, 9:1871–1874, 2008.
- [7] Q. Ho, J. Cipar, H. Cui, J.-K. Kim, S. Lee, P. B. Gibbons, G. Gibson, G. R. Ganger, and E. P. Xing. More effective distributed ml via a stale synchronous parallel parameter server. In *NIPS*, 2013.
- [8] Kwangmoo Koh, Seung-Jean Kim, and Stephen P Boyd. An interior-point method for large-scale l1-regularized logistic regression. *Journal of Machine learning research*, 8(8):1519–1555, 2007.
- [9] John Langford, Lihong Li, and Tong Zhang. Sparse online learning via truncated gradient. *Journal of Machine Learning Research*, 10:777–801, 2009.
- [10] Ching-Pei Lee and Dan Roth. Distributed box-constrained quadratic optimization for dual linear SVM. In *ICML, Lille, France, 2015*, pages 987–996, 2015. URL <http://jmlr.org/proceedings/papers/v37/leea15.html>.

- [11] Honglak Lee, Roger Grosse, Rajesh Ranganath, and Andrew Y. Ng. Convolutional deep belief networks for scalable unsupervised learning of hierarchical representations. In *ICML*, pages 609–616, 2009.
- [12] Chih-Jen Lin and Jorge J. Moré. Newton’s method for large bound-constrained optimization problems. *SIAM Journal on Optimization*, 9(4):1100–1127, 1999.
- [13] Haipeng Luo, Patrick Haffner, and Jean-François Paiement. Accelerated parallel optimization methods for large scale machine learning. *arXiv:1411.6725*, 2014.
- [14] Jakub Marecek, Peter Richtárik, and Martin Takáč. Distributed block coordinate descent for minimizing partially separable functions. *arXiv:1406.0238*, 2014.
- [15] Andrew Y. Ng. Feature selection, l1 vs. l2 regularization, and rotational invariance. In *ICML*, pages 78–85, 2004.
- [16] Feng Niu, Benjamin Recht, Christopher Re, and Stephen J. Wright. Hogwild: A lock-free approach to parallelizing stochastic gradient descent. In *NIPS*, pages 693–701, 2011.
- [17] Peter Richtárik and Martin Takáč. Parallel coordinate descent methods for big data optimization. *CoRR*, abs/1212.0873, 2012.
- [18] Peter Richtárik and Martin Takáč. Distributed coordinate descent method for learning with big data. *arXiv:1310.2059*, 2013.
- [19] Chad Scherrer, Mahantesh Halappanavar, Ambuj Tewari, and David Haglin. Scaling up coordinate descent algorithms for large l1-regularization problems. In *ICML*, 2012. URL <http://icml.cc/discuss/2012/705.html>.
- [20] Chad Scherrer, Ambuj Tewari, Mahantesh Halappanavar, and David Haglin. Feature clustering for accelerating parallel coordinate descent. In *NIPS*, pages 28–36, 2012.
- [21] Shai Shalev-Shwartz and Ambuj Tewari. Stochastic methods for l_1 regularized loss minimization. In *ICML*, pages 117–124, 2009.
- [22] Paul Tseng and Sangwoon Yun. A coordinate gradient descent method for non-smooth separable minimization. *Mathematical Programming*, 117(1-2):387–423, 2009.
- [23] John Wright, Allen Y. Yang, Arvind Ganesh, Shankar S. Sastry, and Yi Ma. Robust face recognition via sparse representation. *IEEE Transactions on Pattern Analysis and Machine Intelligence*, 31(2):210–227, 2009.

- [24] Guo-Xun Yuan, Kai-Wei Chang, Cho-Jui Hsieh, and Chih-Jen Lin. A comparison of optimization methods and software for large-scale l1-regularized linear classification. *Journal of Machine Learning Research*, 11:3183–3234, 2010.
- [25] Guo-Xun Yuan, Chia-Hua Ho, and Chih-Jen Lin. An improved glmnet for l1-regularized logistic regression. In *KDD*, pages 33–41, 2011.
- [26] Martin Zinkevich, Alex Smola, and John Langford. Slow learners are fast. In *NIPS*, pages 2331–2339, 2009.
- [27] Martin Zinkevich, Markus Weimer, Alexander J. Smola, and Lihong Li. Parallelized stochastic gradient descent. In *NIPS*, pages 2595–2603, 2010.

Appendix

A. Full Proofs of Theorems 1 and 2

A.1 Proof of Lemma 1(a)

Proof. (1) We first prove that $\mathbf{E}_{\mathcal{B}^t}[\bar{\lambda}(\mathcal{B}^t)]$ is monotonically increasing with respect to P and $\mathbf{E}_{\mathcal{B}^t}[\bar{\lambda}(\mathcal{B}^t)]$ is constant with respect to P , if λ_i is constant or $\lambda_1 = \lambda_2 = \dots = \lambda_n$.

Let λ_k be the k -th minimum of $(\mathbf{X}^\top \mathbf{X})_{jj}, j = 1, \dots, n$, for $1 \leq P \leq n$. We define

$$\begin{aligned} f(P) &:= \mathbf{E}_{\mathcal{B}^t}[\bar{\lambda}(\mathcal{B}^t)] = \\ &(\lambda_n C_{n-1}^{P-1} + \dots + \lambda_k C_{k-1}^{P-1} + \dots + \lambda_P C_{P-1}^{P-1}) / C_n^P, \end{aligned} \quad (19)$$

where C_n^P is a binomial coefficient. For $1 \leq P \leq n-1$,

$$\begin{aligned} &f(P+1) - f(P) \\ &= -\lambda_P \frac{C_{P-1}^{P-1}}{C_n^P} + \sum_{k=n}^{P+1} \lambda_k \left(\frac{C_{k-1}^P}{C_n^{P+1}} - \frac{C_{k-1}^{P-1}}{C_n^P} \right) \\ &= -\lambda_P \frac{C_{P-1}^{P-1}}{C_n^P} + \sum_{k=n}^{P+1} \lambda_k \frac{(P+1)k - P(n+1)}{P(n-P)} \frac{C_{k-1}^{P-1}}{C_n^P}. \end{aligned}$$

When $\bar{k} = \lceil \frac{(P+1)k}{P(n+1)} \rceil$, then $(P+1)k - P(n+1) \geq 0, \forall k \geq \bar{k}$, and $(P+1)k - P(n+1) \leq 0, \forall k < \bar{k}$. The above equation is equivalent to

$$\begin{aligned} &f(P+1) - f(P) = \\ &\left[\sum_{k=n}^{\bar{k}} \lambda_k \frac{(P+1)k - P(n+1)}{P(n-P)} \frac{C_{k-1}^{P-1}}{C_n^P} \right] - \\ &\left[\sum_{k=\bar{k}}^{P+1} \lambda_k \frac{P(n+1) - (P+1)k}{P(n-P)} \frac{C_{k-1}^{P-1}}{C_n^P} \right] - \lambda_P \frac{C_{P-1}^{P-1}}{C_n^P}. \end{aligned}$$

According to the observations that $\lambda_k \geq \lambda_{\bar{k}}, \forall k \geq \bar{k}$ and $\lambda_k \leq \lambda_{\bar{k}}, \forall k < \bar{k}$, we can decrease the above equation by substitute λ_k by $\lambda_{\bar{k}}$. That is,

$$\begin{aligned} &f(P+1) - f(P) \\ &\geq \left[\sum_{k=n}^{\bar{k}} \lambda_{\bar{k}} \frac{(P+1)k - P(n+1)}{P(n-P)} \frac{C_{k-1}^{P-1}}{C_n^P} \right] - \\ &\left[\sum_{k=\bar{k}}^{P+1} \lambda_{\bar{k}} \frac{P(n+1) - (P+1)k}{P(n-P)} \frac{C_{k-1}^{P-1}}{C_n^P} \right] - \lambda_{\bar{k}} \frac{C_{P-1}^{P-1}}{C_n^P} \end{aligned}$$

$$\begin{aligned}
&= \lambda_{\bar{k}} \left[-\frac{C_{P-1}^{P-1}}{C_n^P} + \sum_{k=n}^{P+1} \frac{(P+1)k - P(n+1)}{P(n-P)} \frac{C_{k-1}^{P-1}}{C_n^P} \right] \\
&= \lambda_{\bar{k}} \left[-\frac{C_{P-1}^{P-1}}{C_n^P} + \sum_{k=n}^{P+1} \left(\frac{C_{k-1}^P}{C_n^{P+1}} - \frac{C_{k-1}^{P-1}}{C_n^P} \right) \right] \\
&= \lambda_{\bar{k}} \left[\sum_{k=n}^{P+1} \frac{C_{k-1}^P}{C_n^{P+1}} - \sum_{k=n}^P \frac{C_{k-1}^{P-1}}{C_n^P} \right] \\
&= \lambda_{\bar{k}} [1 - 1] = 0
\end{aligned}$$

Thus, $f(P+1) - f(P) \geq 0, \forall 1 \leq P \leq n-1$. Namely, $\mathbf{E}_{\mathcal{B}^t} \bar{\lambda}(\mathcal{B}^t)$ is monotonically increasing with respect to P . Clearly, from (19), if $\lambda_1 = \lambda_2 = \dots = \lambda_n$, then $\mathbf{E}_{\mathcal{B}^t} [\bar{\lambda}(\mathcal{B}^t)] = \lambda_1$, which is constant with respect to P .

(2) Next, we prove that $\mathbf{E}_{\mathcal{B}^t} [\bar{\lambda}(\mathcal{B}^t)]/P$ is monotonically decreasing with respect to P . Let λ_k be the k -th minimum of $(\mathbf{X}^\top \mathbf{X})_{jj}, j = 1, \dots, n$. For $1 \leq P \leq n$, define

$$\begin{aligned}
g(P) &:= \frac{\mathbf{E}_{\mathcal{B}^t} [\bar{\lambda}(\mathcal{B}^t)]}{P} = \\
&\frac{1}{PC_n^P} (\lambda_n C_{n-1}^{P-1} + \dots + \lambda_k C_{k-1}^{P-1} + \dots + \lambda_P C_{P-1}^{P-1}).
\end{aligned}$$

For $1 \leq P \leq n-1$, we have

$$\begin{aligned}
&g(P+1) - g(P) \\
&= -\lambda_P \frac{C_{P-1}^{P-1}}{PC_n^P} + \sum_{k=n}^{P+1} \lambda_k \left(\frac{C_{k-1}^P}{(P+1)C_n^{P+1}} - \frac{C_{k-1}^{P-1}}{PC_n^P} \right) \\
&= -\lambda_P \frac{C_{P-1}^{P-1}}{PC_n^P} + \sum_{k=n}^{P+1} \lambda_k \frac{k-n}{n-P} \frac{C_{k-1}^{P-1}}{PC_n^P}.
\end{aligned}$$

According to the observations that $\frac{k-n}{n-P} \leq 0$ and $\lambda_k \geq \lambda_P, \forall k = n, \dots, P+1$, we can increase the above equation by substituting λ_k with λ_P . That is

$$\begin{aligned}
&g(P+1) - g(P) \\
&\leq -\lambda_P \frac{C_{P-1}^{P-1}}{PC_n^P} + \sum_{k=n}^{P+1} \lambda_P \frac{k-n}{n-P} \frac{C_{k-1}^{P-1}}{PC_n^P} \\
&= \lambda_P \left[-\frac{C_{P-1}^{P-1}}{PC_n^P} + \sum_{k=n}^{P+1} \frac{k-n}{n-P} \frac{C_{k-1}^{P-1}}{PC_n^P} \lambda_P \right] \\
&= \lambda_P \left[\frac{C_{P-1}^{P-1}}{PC_n^P} + \sum_{k=n}^{P+1} \left(\frac{C_{k-1}^P}{(P+1)C_n^{P+1}} - \frac{C_{k-1}^{P-1}}{PC_n^P} \right) \right]
\end{aligned}$$

$$\begin{aligned}
&= \lambda_P \left[\frac{1}{P+1} \sum_{k=n}^{P+1} \frac{C_{k-1}^P}{C_n^{P+1}} - \frac{1}{P} \sum_{k=n}^P \frac{C_{k-1}^{P-1}}{C_n^P} \right] \\
&= \lambda_P \left[\frac{1}{P+1} - \frac{1}{P} \right] \\
&\leq 0,
\end{aligned} \tag{20}$$

where (20) comes from $\lambda_P \geq 0$ and $\frac{1}{P+1} - \frac{1}{P} < 0$. Thus, $g(P+1) - g(P) \leq 0, \forall 1 \leq P \leq n-1$. Namely, $\frac{\mathbf{E}_{\mathcal{B}^t}[\bar{\lambda}(\mathcal{B}^t)]}{P}$ is monotonically decreasing with respect to P . ■

A.2 Proof of Lemma 1(b)

Proof. (1) For logistic regression,

$$\nabla_{jj}^2 L(\mathbf{w}) = c \sum_{i=1}^s \tau(y_i \mathbf{w}^\top \mathbf{x}_i) (1 - \tau(y_i \mathbf{w}^\top \mathbf{x}_i)) x_{ij}^2, \tag{21}$$

where $\tau(s) \equiv \frac{1}{1+e^{-s}}$ is the derivative of the logistic loss function $\log(1+e^s)$. Because $0 < \tau(s) < 1$, we have $0 < \nabla_{jj}^2 L(\mathbf{w}) \leq \frac{1}{4} c \sum_{i=1}^s x_{ij}^2 = \frac{1}{4} c (\mathbf{X}^\top \mathbf{X})_{jj}$ (the equal sign holds when $\tau(s) = \frac{1}{2}$), and thus (12) holds when $\theta = \frac{1}{4}$ for logistic regression. As $\bar{\lambda}(\mathcal{N})$ is the maximum element of $(\mathbf{X}^\top \mathbf{X})_{jj}$ where $j \in \mathcal{N}$, $\nabla_{jj}^2 L(\mathbf{w}) \leq \bar{h} = \theta c \bar{\lambda}(\mathcal{N})$ in (13) also holds. In addition, because in practice $|y_i \mathbf{w}^\top \mathbf{x}_i| < \infty$, there exist $\bar{\tau}$ and $\underline{\tau}$ such that $0 < \underline{\tau} \leq \tau(y_i \mathbf{w}^\top \mathbf{x}_i) \leq \bar{\tau} < 1$. Thus, there exists a $\underline{h} > 0$ such that $0 < \underline{h} \leq \nabla_{jj}^2 L(\mathbf{w})$.

(2) For L_2 -loss SVM, use generalized second derivative

$$2c \sum_{i \in I(\mathbf{w})} x_{ij}^2 \leq 2c \sum_{i=1}^s x_{ij}^2 = 2c (\mathbf{X}^\top \mathbf{X})_{jj}, \tag{22}$$

where $I(\mathbf{w}) = \{i \mid y_i \mathbf{w}^\top \mathbf{x}_i < 1\}$. So (12) holds for $\theta = 2$ for L_2 -loss SVM. Because $\bar{\lambda}(\mathcal{N})$ is the maximum element of $(\mathbf{X}^\top \mathbf{X})_{jj}$ where $j \in \mathcal{N}$, so $\nabla_{jj}^2 L(\mathbf{w}) \leq \bar{h} = \theta c \bar{\lambda}(\mathcal{N})$ in (13) also holds. To ensure that $\nabla_{jj}^2 L(\mathbf{w}) > 0$, a very small positive number ν ($\nu = 10^{-12}$) is added when $\nabla_{jj}^2 L(\mathbf{w}) \leq 0$ according to [4]. Thus, $\underline{h} = \nu > 0$. ■

A.3 Proof of Lemma 1(c)

Proof. We follow the proof in [22], from (4) and the convexity of L_1 -norm, for any $\alpha \in (0, 1)$,

$$\begin{aligned}
&\nabla L(\mathbf{w})^\top \mathbf{d} + \frac{1}{2} \mathbf{d}^\top \mathbf{H} \mathbf{d} + \|\mathbf{w} + \mathbf{d}\|_1 \\
&\leq \nabla L(\mathbf{w})^\top (\alpha \mathbf{d}) + \frac{1}{2} (\alpha \mathbf{d})^\top \mathbf{H} (\alpha \mathbf{d}) + \|\mathbf{w} + (\alpha \mathbf{d})\|_1 \\
&= \alpha \nabla L(\mathbf{w})^\top \mathbf{d} + \frac{1}{2} \alpha^2 \mathbf{d}^\top \mathbf{H} \mathbf{d} + \|\alpha(\mathbf{w} + \mathbf{d}) + (1-\alpha)\mathbf{w}\|_1 \\
&\leq \alpha \nabla L(\mathbf{w})^\top \mathbf{d} + \frac{1}{2} \alpha^2 \mathbf{d}^\top \mathbf{H} \mathbf{d} + \alpha \|\mathbf{w} + \mathbf{d}\|_1 + (1-\alpha) \|\mathbf{w}\|_1.
\end{aligned}$$

After rearranging these terms, we have

$$\begin{aligned} & (1 - \alpha)\nabla L(\mathbf{w})^\top \mathbf{d} + (1 - \alpha)(\|\mathbf{w} + \mathbf{d}\|_1 - \|\mathbf{w}\|_1) \\ & \leq -\frac{1}{2}(1 - \alpha)(1 + \alpha)\mathbf{d}^\top \mathbf{H}\mathbf{d}. \end{aligned}$$

Dividing both sides by $1 - \alpha > 0$ and taking α infinitely approaching 0 yields

$$\nabla L(\mathbf{w})^\top \mathbf{d} + \|\mathbf{w} + \mathbf{d}\|_1 - \|\mathbf{w}\|_1 \leq -\mathbf{d}^\top \mathbf{H}\mathbf{d},$$

and thus

$$\begin{aligned} \Delta & = \nabla L(\mathbf{w})^\top \mathbf{d} + \gamma \mathbf{d}^\top \mathbf{H}\mathbf{d} + \|\mathbf{w} + \mathbf{d}\|_1 - \|\mathbf{w}\|_1 \\ & \leq (\gamma - 1)\mathbf{d}^\top \mathbf{H}\mathbf{d}, \end{aligned} \tag{23}$$

which proves (14). From the Armijo rule in (6) we have

$$F(\mathbf{w} + \alpha \mathbf{d}) - F(\mathbf{w}) \leq \sigma \alpha \Delta.$$

By substituting (23) into the above equation and considering that $\gamma \in [0, 1)$ we obtain

$$F(\mathbf{w} + \alpha \mathbf{d}) - F(\mathbf{w}) \leq \sigma \alpha (\gamma - 1) \mathbf{d}^\top \mathbf{H}\mathbf{d} \leq 0.$$

Hence $\{F(\mathbf{w}^t)\}$ is nonincreasing. ■

A.4 Proof of Theorem 1: Convergence of P -dimensional line search

Proof. (1) First, we prove that the descent condition in (6) $F(\mathbf{w} + \alpha \mathbf{d}) - F(\mathbf{w}) \leq \sigma \alpha \Delta$ is satisfied for any $\sigma \in (0, 1)$ whenever $0 \leq \alpha \leq \min \left\{ 1, \frac{2h(1-\sigma+\sigma\gamma)}{\theta c \sqrt{P\lambda(\mathcal{B}^t)}} \right\}$.

For any $\alpha \in [0, 1]$,

$$\begin{aligned} & F(\mathbf{w} + \alpha \mathbf{d}) - F(\mathbf{w}) \\ & = L(\mathbf{w} + \alpha \mathbf{d}) - L(\mathbf{w}) + \|\mathbf{w} + \alpha \mathbf{d}\|_1 - \|\mathbf{w}\|_1 \\ & = \int_0^1 \nabla L(\mathbf{w} + u\alpha \mathbf{d})^\top (\alpha \mathbf{d}) du \end{aligned} \tag{24}$$

$$\begin{aligned} & + \|\mathbf{w} + \alpha \mathbf{d}\|_1 - \|\mathbf{w}\|_1 \\ & = \alpha \nabla L(\mathbf{w})^\top \mathbf{d} + \|\mathbf{w} + \alpha \mathbf{d}\|_1 - \|\mathbf{w}\|_1 \\ & + \int_0^1 (\nabla L(\mathbf{w} + u\alpha \mathbf{d}) - \nabla L(\mathbf{w}))^\top (\alpha \mathbf{d}) du, \end{aligned} \tag{25}$$

where (24) is based on the definition of definite integration. Because in the t -th iteration of PCDN, $d_j = 0, \forall j \notin \mathcal{B}^t$, we define auxiliary matrix $\mathbf{G} \in \mathbb{R}^{n \times n}$ such that $g_{jj} = 1, \forall j \in \mathcal{B}^t$, otherwise $g_{jj} = 0$. Then we have

$$\begin{aligned} & (\nabla L(\mathbf{w} + u\alpha \mathbf{d}) - \nabla L(\mathbf{w}))^\top (\alpha \mathbf{d}) = \\ & (\mathbf{G} \cdot (\nabla L(\mathbf{w} + u\alpha \mathbf{d}) - \nabla L(\mathbf{w})))^\top (\alpha \mathbf{d}). \end{aligned} \tag{26}$$

Substituting (26) into (25) we obtain

$$\begin{aligned}
& F(\mathbf{w} + \alpha \mathbf{d}) - F(\mathbf{w}) \\
&= \alpha \nabla L(\mathbf{w})^\top \mathbf{d} + \|\mathbf{w} + \alpha \mathbf{d}\|_1 - \|\mathbf{w}\|_1 + \\
& \int_0^1 (\mathbf{G} \cdot (\nabla L(\mathbf{w} + u\alpha \mathbf{d}) - \nabla L(\mathbf{w})))^\top (\alpha \mathbf{d}) du \\
& \leq \alpha \nabla L(\mathbf{w})^\top \mathbf{d} + \alpha (\|\mathbf{w} + \mathbf{d}\|_1 - \|\mathbf{w}\|_1) + \\
& \alpha \int_0^1 \|\mathbf{G} \cdot (\nabla L(\mathbf{w} + u\alpha \mathbf{d}) - \nabla L(\mathbf{w}))\| \|\mathbf{d}\| du, \tag{27}
\end{aligned}$$

where (27) is from the convexity of L_1 -norm and the Cauchy-Schwarz inequality. It follows that

$$\begin{aligned}
& \|\mathbf{G} \cdot (\nabla L(\mathbf{w} + u\alpha \mathbf{d}) - \nabla L(\mathbf{w}))\| \\
&= \sqrt{\sum_{j \in \mathcal{B}^t} (\nabla L(\mathbf{w} + u\alpha \mathbf{d}) - \nabla L(\mathbf{w}))^2} \\
&\leq u\alpha \sqrt{\sum_{j \in \mathcal{B}^t} (\nabla_{jj}^2 L(\bar{\mathbf{w}}))^2} \|\mathbf{d}\| \\
&\leq u\alpha \sqrt{P(\theta c \bar{\lambda}(\mathcal{B}^t))^2} \|\mathbf{d}\| \\
&= u\alpha \theta c \sqrt{P \bar{\lambda}(\mathcal{B}^t)} \|\mathbf{d}\|, \tag{28}
\end{aligned}$$

where $\bar{\mathbf{w}} = v(\mathbf{w} + u\alpha \mathbf{d}) + (1-v)\mathbf{w}$, $0 \leq v \leq 1$. We note (28) results from Lemma 1(b). By substituting the above inequality into (27) we have

$$\begin{aligned}
& F(\mathbf{w} + \alpha \mathbf{d}) - F(\mathbf{w}) \\
&\leq \alpha \nabla L(\mathbf{w})^\top \mathbf{d} + \alpha (\|\mathbf{w} + \mathbf{d}\|_1 - \|\mathbf{w}\|_1) + \\
& \alpha^2 \theta c \sqrt{P \bar{\lambda}(\mathcal{B}^t)} \int_0^1 u \|\mathbf{d}\|^2 dt \\
&= \alpha \nabla L(\mathbf{w})^\top \mathbf{d} + \|\mathbf{w} + \mathbf{d}\|_1 - \|\mathbf{w}\|_1 + \\
& \frac{\alpha^2 \theta c \sqrt{P \bar{\lambda}(\mathcal{B}^t)}}{2} \|\mathbf{d}\|^2 \\
&= \alpha \nabla L(\mathbf{w})^\top \mathbf{d} + \gamma \mathbf{d}^\top \mathbf{H} \mathbf{d} + \|\mathbf{w} + \mathbf{d}\|_1 - \|\mathbf{w}\|_1 + \\
& \frac{\alpha^2 \theta c \sqrt{P \bar{\lambda}(\mathcal{B}^t)}}{2} \|\mathbf{d}\|^2 - \alpha \gamma \mathbf{d}^\top \mathbf{H} \mathbf{d} \\
&= \alpha \Delta + \frac{\alpha^2 \theta c \sqrt{P \bar{\lambda}(\mathcal{B}^t)}}{2} \|\mathbf{d}\|^2 - \alpha \gamma \mathbf{d}^\top \mathbf{H} \mathbf{d}. \tag{29}
\end{aligned}$$

If we set $\alpha \leq \frac{2h(1-\sigma+\sigma\gamma)}{\theta c \sqrt{P \bar{\lambda}(\mathcal{B}^t)}}$, then

$$\begin{aligned}
& \frac{\alpha^2 \theta c \sqrt{P \bar{\lambda}(\mathcal{B}^t)}}{2} \|\mathbf{d}\|^2 - \alpha \gamma \mathbf{d}^\top \mathbf{H} \mathbf{d} \\
& \leq \alpha (\underline{h}(1 - \sigma + \sigma \gamma) \|\mathbf{d}\|^2 - \gamma \mathbf{d}^\top \mathbf{H} \mathbf{d}) \\
& \leq \alpha ((1 - \sigma + \sigma \gamma) \mathbf{d}^\top \mathbf{H} \mathbf{d} - \gamma \mathbf{d}^\top \mathbf{H} \mathbf{d}) \tag{30} \\
& = \alpha (1 - \sigma)(1 - \gamma) \mathbf{d}^\top \mathbf{H} \mathbf{d} \\
& \leq -\alpha (1 - \sigma) \Delta, \tag{31}
\end{aligned}$$

where (30) comes from (13) in Lemma 1(b) and (31) is based on Lemma 1(c). The above equation together with (29) proves that $F(\mathbf{w} + \alpha \mathbf{d}) - F(\mathbf{w}) \leq \sigma \alpha \Delta$ if $\alpha \leq \frac{2\underline{h}(1-\sigma+\sigma\gamma)}{\theta c \sqrt{P \bar{\lambda}(\mathcal{B}^t)}}$.

(2) We prove the upper bound of $\mathbf{E}[q^t]$. In the Armijo line search procedure, it tests different values of α from larger to smaller, and stops right after finding one value that satisfy $F(\mathbf{w}^t + \alpha^t \mathbf{d}^t) - F(\mathbf{w}^t) \leq \sigma \alpha^t \Delta^t$. Thus in the t -th iteration, the chosen step size α^t satisfies

$$\alpha^t \geq \frac{2\underline{h}(1 - \sigma + \sigma \gamma)}{\theta c \sqrt{P \bar{\lambda}(\mathcal{B}^t)}}. \tag{32}$$

From (6) we have $\alpha^t = \beta^q$, and thus the line search step number of the t -th iteration q^t

$$q^t = 1 + \log_{\beta} \alpha^t \leq 1 + \log_{\beta^{-1}} \frac{\theta c \sqrt{P \bar{\lambda}(\mathcal{B}^t)}}{2\underline{h}(1 - \sigma + \sigma \gamma)}. \tag{33}$$

Taking expectation on both sides with respect to the random choices of \mathcal{B}^t , we obtain

$$\begin{aligned}
\mathbf{E}[q^t] & \leq 1 + \log_{\beta^{-1}} \frac{\theta c}{2\underline{h}(1 - \sigma + \sigma \gamma)} + \frac{1}{2} \log_{\beta^{-1}} P + \\
& \quad \mathbf{E}_{\mathcal{B}^t} [\log_{\beta^{-1}} \bar{\lambda}(\mathcal{B}^t)] \\
& \leq 1 + \log_{\beta^{-1}} \frac{\theta c}{2\underline{h}(1 - \sigma + \sigma \gamma)} + \frac{1}{2} \log_{\beta^{-1}} P + \\
& \quad \log_{\beta^{-1}} \mathbf{E}_{\mathcal{B}^t} [\bar{\lambda}(\mathcal{B}^t)], \tag{34}
\end{aligned}$$

where (34) is based on Jensen's inequality for concave function $\log_{\beta^{-1}}(\cdot)$. ■

A.5 Proof of Global convergence

Proof. (1) We first relate PCDN to the framework in [22]. Note that the selection of bundle \mathcal{B}^t in (8) is consistent with that used in CGD (i.e., (12) in [22]). For the descent direction computed in a bundle in Algorithm 3, we have

$$\mathbf{d}^t = \sum_{j \in \mathcal{B}^t} d(\mathbf{w}^t; j) \mathbf{e}_j$$

$$= \sum_{j \in \mathcal{B}^t} \arg \min_d \{ \nabla_j L(\mathbf{w}^t)^\top d + \frac{1}{2} \nabla_{jj}^2 L(\mathbf{w}^t) d^2 + |w_j^t + d| \} \mathbf{e}_j \quad (35)$$

$$= \arg \min_{\mathbf{d}} \left\{ \sum_{j \in \mathcal{B}^t} (\nabla_j L(\mathbf{w}^t)^\top d_j + \frac{1}{2} \nabla_{jj}^2 L(\mathbf{w}^t) d_j^2 + |w_j^t + d_j|) \right. \\ \left. \mid d_j = 0, \forall j \notin \mathcal{B}^t \right\} \\ = \arg \min_{\mathbf{d}} \left\{ \nabla L(\mathbf{w}^t)^\top \mathbf{d} + \frac{1}{2} \mathbf{d}^\top \mathbf{H} \mathbf{d} + \|\mathbf{w} + \mathbf{d}\|_1 \right. \\ \left. \mid d_j = 0, \forall j \notin \mathcal{B}^t \right\} \quad (36)$$

$$\equiv \mathbf{d}_{\mathbf{H}}(\mathbf{w}^t; \mathcal{B}^t), \quad (37)$$

where (35) is derived by considering the definition of $d(\mathbf{w}; j)$ in (4); (36) is obtained by applying the setting of $\mathbf{H} \equiv \text{diag}(\nabla^2 L(\mathbf{w}))$; (37) is defined by following the descent direction definition of Tseng et al. (i.e., (6) in [22]). Therefore the definition of direction computed is in a manner similar to CGD. Furthermore, since PCDN uses the Armijo line search for \mathbf{d}^t , by taking $\mathbf{H} \equiv \text{diag}(\nabla^2 L(\mathbf{w}))$, it is clear that we can use the framework in [22] to analyze the global convergence of PCDN.

(2) We use Theorem 1(e) in [22] to prove the global convergence, which requires that $\{\mathcal{B}^t\}$ is chosen under the Gauss-Seidel rule and $\sup_t \alpha^t < \infty$. In (6), $\alpha^t \leq 1, t = 1, 2, \dots$, which satisfies $\sup_t \alpha^t < \infty$. To ensure global convergence, Tseng et al. make the following assumption,

$$0 < \underline{h} \leq \nabla_{jj}^2 L(\mathbf{w}^t) \leq \bar{h}, \quad \forall j = 1, \dots, n, t = 0, 1, \dots$$

which is fulfilled by Lemma 1(b). According to Theorem 1(e) in [22], any cluster point of $\{\mathbf{w}^t\}$ is a stationary point of $F(\mathbf{w})$. ■

A.6 Proof of Theorem 2: Convergence rate

To analyze the convergence rate, we transform (1) into an equivalent problem with a twice differentiable regularizer following [21]. Let $\hat{\mathbf{w}} \in \mathbb{R}_+^{2n}$ with duplicated features⁹ $\hat{\mathbf{x}}_i \equiv [\mathbf{x}_i; -\mathbf{x}_i] \in \mathbb{R}^{2n}$, the problem becomes

$$\min_{\hat{\mathbf{w}} \in \mathbb{R}_+^{2n}} F(\hat{\mathbf{w}}) \equiv c \sum_{i=1}^s \varphi(\hat{\mathbf{w}}; \hat{\mathbf{x}}_i, y_i) + \sum_{j=1}^{2n} \hat{\mathbf{w}}_j. \quad (38)$$

The descent direction is computed by

$$\hat{d}_j = \hat{d}(\hat{\mathbf{w}}; j) \equiv \\ \arg \min_{\hat{d}} \left\{ \nabla_j L(\hat{\mathbf{w}}) \hat{d} + \frac{1}{2} \nabla_{jj}^2 L(\hat{\mathbf{w}}) \hat{d}^2 + \hat{w}_j + \hat{d} \right\} \quad (39) \\ = -(\nabla_j L(\hat{\mathbf{w}}) + 1) / \nabla_{jj}^2 L(\hat{\mathbf{w}}).$$

9. Although our analysis uses duplicate features, they are not required for an implementation.

In the following proof we omit the “ \wedge ” above each variables for ease of presentation.

Proof. Assume that \mathbf{w}^* minimizes the objective in (38). Define the potential function as

$$\begin{aligned}\Psi(\mathbf{w}) &\equiv \\ &\frac{\theta c \bar{\lambda}(\mathcal{B}^t)}{2} \|\mathbf{w} - \mathbf{w}^*\|^2 + \frac{\theta c \bar{\lambda}(\mathcal{B}^t) \sup_t \alpha^t}{2\sigma(1-\gamma)\underline{h}} F(\mathbf{w}) \\ &= a \|\mathbf{w} - \mathbf{w}^*\|^2 + b F(\mathbf{w}),\end{aligned}\tag{40}$$

where

$$a = \frac{\theta c \bar{\lambda}(\mathcal{B}^t)}{2}, \quad b = \frac{\theta c \bar{\lambda}(\mathcal{B}^t) \sup_t \alpha^t}{2\sigma(1-\gamma)\underline{h}}.$$

Thus, we have

$$\begin{aligned}\Psi(\mathbf{w}) - \Psi(\mathbf{w} + \alpha \mathbf{d}) &= \\ &a(\|\mathbf{w} - \mathbf{w}^*\|^2 - \|\mathbf{w} + \alpha \mathbf{d} - \mathbf{w}^*\|^2) + b(F(\mathbf{w}) - F(\mathbf{w} + \alpha \mathbf{d})) \\ &= a\alpha(-2\mathbf{w}^\top \mathbf{d} + 2\mathbf{w}^{*\top} \mathbf{d} - \alpha \mathbf{d}^\top \mathbf{d}) + b(F(\mathbf{w}) - F(\mathbf{w} + \alpha \mathbf{d})) \\ &\geq a\alpha(-2\mathbf{w}^\top \mathbf{d} + 2\mathbf{w}^{*\top} \mathbf{d} - \alpha \mathbf{d}^\top \mathbf{d}) + b\sigma\alpha(1-\gamma)\mathbf{d}^\top \mathbf{H} \mathbf{d},\end{aligned}\tag{41}$$

where (41) uses (14) and (15) in Lemma 1(c). Using the fact that $d_j = 0, \forall j \notin \mathcal{B}^t$, we derive from (41) that

$$\begin{aligned}\Psi(\mathbf{w}) - \Psi(\mathbf{w} + \alpha \mathbf{d}) &\geq \sum_{j \in \mathcal{B}^t} a\alpha(-2w_j d_j + 2w_j^* d_j - \alpha d_j^2) + b\sigma\alpha(1-\gamma)\nabla_{jj}^2 L(\mathbf{w}) d_j^2 \\ &= \sum_{j \in \mathcal{B}^t} a\alpha(-2w_j d_j + 2w_j^* d_j) + \alpha[b\sigma(1-\gamma)\nabla_{jj}^2 L(\mathbf{w}) - a\alpha] d_j^2 \\ &\geq \sum_{j \in \mathcal{B}^t} a\alpha(-2w_j + 2w_j^*) d_j,\end{aligned}\tag{42}$$

and (42) uses the fact that

$$\begin{aligned}&b\sigma(1-\gamma)\nabla_{jj}^2 L(\mathbf{w}) - a\alpha \\ &= \frac{\theta c \bar{\lambda}(\mathcal{B}^t)}{2} \left[\frac{\nabla_{jj}^2 L(\mathbf{w}) \sup_t \alpha^t}{\underline{h}} - \alpha \right] \\ &\geq \frac{\theta c \bar{\lambda}(\mathcal{B}^t)}{2} (\sup_t \alpha^t - \alpha) \geq 0.\end{aligned}$$

By substituting $a = \frac{\theta c \bar{\lambda}(\mathcal{B}^t)}{2}$ and $d_j = -(\nabla_j L(\mathbf{w}) + 1)/\nabla_{jj}^2 L(\mathbf{w})$ (See (39)) into (42), we have the following equations

$$\Psi(\mathbf{w}) - \Psi(\mathbf{w} + \alpha \mathbf{d})$$

$$\geq \sum_{j \in \mathcal{B}^t} \frac{\theta c \bar{\lambda}(\mathcal{B}^t) \alpha}{\nabla_{jj}^2 L(\mathbf{w})} (w_j - w_j^*) (\nabla_j L(\mathbf{w}) + 1) \quad (43)$$

$$\geq \sum_{j \in \mathcal{B}^t} \frac{\bar{\lambda}(\mathcal{B}^t) \alpha}{(\mathbf{X}^\top \mathbf{X})_{jj}} (w_j - w_j^*) (\nabla_j L(\mathbf{w}) + 1) \quad (44)$$

$$\geq \alpha \sum_{j \in \mathcal{B}^t} (w_j - w_j^*) (\nabla_j L(\mathbf{w}) + 1). \quad (45)$$

We note (44) is based on Lemma 1(b) and (45) results from the definition of $\bar{\lambda}(\mathcal{B}^t)$.

Taking the expectation with respect to the random choices of \mathcal{B}^t on both sides of (45) we have

$$\begin{aligned} & \mathbf{E}_{\mathcal{B}^t} [\Psi(\mathbf{w}) - \Psi(\mathbf{w} + \alpha \mathbf{d})] \\ & \geq \inf_t \alpha^t \mathbf{E}_{\mathcal{B}^t} \left[\sum_{j \in \mathcal{B}^t} (w_j - w_j^*) (\nabla_j L(\mathbf{w}) + 1) \right] \\ & = \inf_t \alpha^t P \mathbf{E}_j [(w_j - w_j^*) (\nabla_j L(\mathbf{w}) + 1)] \\ & = \inf_t \alpha^t \frac{P}{2n} (\mathbf{w} - \mathbf{w}^*) (\nabla L(\mathbf{w}) + \mathbf{1}) \\ & \geq \inf_t \alpha^t \frac{P}{2n} (F(\mathbf{w}) - F(\mathbf{w}^*)), \end{aligned} \quad (46)$$

where (46) comes from the convexity of $L(\mathbf{w})$.

By summing over $T + 1$ iterations on both sides of (46), with an expectation over the random choices of \mathcal{B}^t , we obtain,

$$\begin{aligned} & \mathbf{E} \left[\sum_{t=0}^T \Psi(\mathbf{w}^t) - \Psi(\mathbf{w}^{t+1}) \right] \\ & \geq \inf_t \alpha^t \frac{P}{2n} \mathbf{E} \left[\sum_{t=0}^T F(\mathbf{w}^t) - F(\mathbf{w}^*) \right] \\ & = \inf_t \alpha^t \frac{P}{2n} [\mathbf{E} \sum_{t=0}^T [F(\mathbf{w}^t)] - (T + 1) F(\mathbf{w}^*)] \\ & \geq \inf_t \alpha^t \frac{P(T + 1)}{2n} [\mathbf{E}[F(\mathbf{w}^\top)] - F(\mathbf{w}^*)], \end{aligned} \quad (47)$$

where (47) comes from Lemma 1(c) that $\{F(\mathbf{w}^t)\}$ is nonincreasing. From (32) we can bound α^t by some positive constant $\xi = \frac{2h(1-\sigma+\sigma\gamma)}{\theta c \sqrt{P \bar{\lambda}(\mathcal{B}^t)}}$,

$$0 < \xi \leq \alpha^t \leq 1. \quad (48)$$

Substituting (48) into (47), we have

$$\mathbf{E} \left[\sum_{t=0}^T \Psi(\mathbf{w}^t) - \Psi(\mathbf{w}^{t+1}) \right] \geq \xi \frac{P(T + 1)}{2n} [\mathbf{E}[F(\mathbf{w}^\top)] - F(\mathbf{w}^*)].$$

By rearranging the above inequality, we have

$$\begin{aligned}
& \mathbf{E}[F(\mathbf{w}^\top)] - F(\mathbf{w}^*) \\
& \leq \frac{2n}{\xi P(T+1)} \mathbf{E}\left[\sum_{t=0}^{\top} \Psi(\mathbf{w}^t) - \Psi(\mathbf{w}^{t+1})\right] \\
& \leq \frac{2n}{\xi P(T+1)} \mathbf{E}[\Psi(\mathbf{w}^0) - \Psi(\mathbf{w}^{T+1})] \\
& \leq \frac{2n}{\xi P(T+1)} \mathbf{E}[\Psi(\mathbf{w}^0)] \tag{49}
\end{aligned}$$

$$= \frac{2n \mathbf{E}_{\mathcal{B}^t} \bar{\lambda}(\mathcal{B}^t)}{\xi P(T+1)} \left[\frac{\theta_c}{2} (\|\mathbf{w}^*\|^2) + \frac{\theta_c \sup_t \alpha^t}{2\sigma(1-\gamma)\underline{h}} (F(\mathbf{0})) \right] \tag{50}$$

$$\leq \frac{2n \mathbf{E}_{\mathcal{B}^t} \bar{\lambda}(\mathcal{B}^t)}{P(T+1)} \cdot \frac{\theta_c}{2\xi} \left[\|\mathbf{w}^*\|^2 + \frac{F(\mathbf{0})}{\sigma(1-\gamma)\underline{h}} \right], \tag{51}$$

where (49) comes from that $\Psi(\mathbf{w}^{T+1}) \geq 0$, and (50) is because \mathbf{w}^0 is set to be $\mathbf{0}$, (51) holds since $\alpha^t \leq 1$. \blacksquare

B. Computational Complexities of PCDN and CDN

The proposed PCDN algorithm takes much less time for each outer iteration than the CDN method. We analyze the computational complexity of PCDN for the k -th outer iteration, $\text{time}(k)$ to demonstrate this point (note that CDN is a special case of PCDN with bundle size $P = 1$).

Let t_{dc} denote the time complexity for computing the descent direction (step 7 in Algorithm 3), and t_{ls} denote the time complexity for a step of P -dimensional line search, which is approximately constant with varying P (See the discussions below). When the computation of descent directions (step 6 in Algorithm 3) is fully parallelized, $\text{time}(k)$ can be estimated by

$$\mathbf{E}[\text{time}(k)] \approx \lceil n/P \rceil \cdot t_{dc} + \lceil n/P \rceil \cdot \mathbf{E}[q^t] \cdot t_{ls}, \tag{52}$$

where the expectation is with respect to the random choice of \mathcal{B}^t , and q^t is the number of line search steps in the t -th iteration. As indicated in (52), the computational complexity of descent directions $\lceil n/P \rceil \cdot t_{dc}$ decreases linearly with the increase of bundle size P . For the cost of Armijo line search, when approximately estimating $\mathbf{E}[q^t]$ by its upper bound in Theorem 1, $\mathbf{E}[q^t]/P$ decreases with respect to P ¹⁰, and thus $\lceil n/P \rceil \cdot \mathbf{E}[q^t] \cdot t_{ls}$ decreases with the increase of bundle size P . The overall computational complexity of PCDN's each outer iteration is lower than that of the CDN method.

10. Using the upper bound in Theorem 1, and the fact that $\mathbf{E}_{\mathcal{B}^t}[\bar{\lambda}(\mathcal{B}^t)]/P$ is monotonically decreasing with respect to P in Lemma 1(a), we can easily obtain this.

We show that the time complexity of one step of P -dimensional line search t_{ls} remains approximately constant with varying bundle size P . The reason being that in each line search step of Algorithm 4, the time complexity remains constant with respect to P . The difference of the whole line search procedure results from computing $\mathbf{d}^\top \mathbf{x}_i = \sum_{j=1}^P d_j x_{ij}$. However, $\mathbf{d}^\top \mathbf{x}_i$ in the PCDN algorithm can be computed in parallel with P threads as well as a reduction-sum operation, and thus the computational complexity remains approximately constant.